AD-A059 546 ROCKWELL INTERNATIONAL COLUMBUS OHIO COLUMBUS AIRCRA--ETC F/G 21/5
VISCID/INVISCID INTERACTION ANALYSIS OF THRUST AUGMENTING EJECT--ETC(U)
FEB 78 P M BEVILAQUA, A D DEJOODE N00014-77-C-0271

UNCLASSIFIED NR78H-21 ONR-CR212-249-1 NL

1 OF
AD
A059546

END
DATE
FILMED
12-78
DDC

LEVEL II

REPORT ONR-CR212-249-1

12

VISCID/INVISCID INTERACTION ANALYSIS OF THRUST AUGMENTING EJECTORS

P. M. Bevilaqua

A. D. DeJoode

Rockwell International
Columbus Aircraft Division
Columbus, Ohio 43216

Contract N00014-77-C-0271
ONR TASK 212-249

28 February 1978

INTERIM REPORT FOR PERIOD 1 JUNE 1977–28 FEBRUARY 1978

Approved for Public Release; Distribution Unlimited.

PREPARED FOR THE

OFFICE OF NAVAL RESEARCH ● 800 N. QUINCY ST. ● ARLINGTON ● VA ● 22217

Change of address

Organizations receiving reports on the initial distribution list should confirm correct address. This list is located at the end of the report. Any change of address or distribution should be conveyed to the Office of Naval Research, Code 211, Arlington, VA 22217.

Disposition

When this report is no longer needed, it may be transmitted to other organizations. Do not return it to the originator or the monitoring office.

Disclaimer

The findings and conclusions contained in this report are not to be construed as an official Department of Defense or Military Department position unless so designated by other official documents.

Reproduction

UNCLASSIFIED

SECURITY CLASSIFICATION OF THIS PAGE (When Data Entered)

REPORT DOCUMENTATION PAGE	READ INSTRUCTIONS BEFORE COMPLETING FORM
1. REPORT NUMBER: ONR CR212-249-1	2. GOVT ACCESSION NO.
3. RECIPIENT'S CATALOG NUMBER	
4. TITLE (and Subtitle): VISCID/INVISCID INTERACTION ANALYSIS OF THRUST AUGMENTING EJECTORS	5. TYPE OF REPORT & PERIOD COVERED: Interim Report 1 June 1977 - 28 Feb. 1978
6. PERFORMING ORG. REPORT NUMBER: NR78H-21	
7. AUTHOR(s): P. M. Bevilaqua, A. D. DeJoode	8. CONTRACT OR GRANT NUMBER(s): N00014-77-C-0271
9. PERFORMING ORGANIZATION NAME AND ADDRESS: Rockwell International, Columbus Aircraft Division, Columbus, Ohio 43216	10. PROGRAM ELEMENT, PROJECT, TASK AREA & WORK UNIT NUMBERS: 62241N, RF41-411-801, NR212-249
11. CONTROLLING OFFICE NAME AND ADDRESS: Office of Naval Research, Vehicle Technology Program (Code 211), Arlington, VA 22217	12. REPORT DATE: 28 February 1978
	13. NUMBER OF PAGES: 44
14. MONITORING AGENCY NAME & ADDRESS (if different from Controlling Office)	15. SECURITY CLASS. (of this report): Unclassified
	15a. DECLASSIFICATION/DOWNGRADING SCHEDULE

16. DISTRIBUTION STATEMENT (of this Report)

Approved for public release, distribution unlimited.

17. DISTRIBUTION STATEMENT (of the abstract entered in Block 20, if different from Report)

18. SUPPLEMENTARY NOTES

19. KEY WORDS (Continue on reverse side if necessary and identify by block number)

ejectors
V/STOL Aerodynamics
turbulence
viscid/inviscid flow interactions
aircraft propulsion
thrust augmentation
panel methods
jet flap diffuser

20. ABSTRACT (Continue on reverse side if necessary and identify by block number)

A method has been developed for calculating the static performance of thrust augmenting ejectors by matching a viscous solution for the flow through the ejector to an inviscid solution for the flow outside the ejector. In effect, the ejector shroud is considered to be "flying" in the secondary velocity field induced by the entrainment of the primary jets. A two-dimensional analysis utilizing a turbulence kinetic energy model for the inner, jet mixing solution and potential flow singularities for the outer, induced flow is described. This approach offers the advantage of including external influences

DD FORM 1 JAN 73 1473 EDITION OF 1 NOV 65 IS OBSOLETE

UNCLASSIFIED

SECURITY CLASSIFICATION OF THIS PAGE (When Data Entered)

20. ABSTRACT (Cont'd)

on the flow through the ejector. Comparisons with data are presented for an ejector having a single central nozzle and Coanda jets on the walls. The accuracy of the matched solution is found to be especially sensitive to the jet flap effect of the flow just downstream of the ejector exit.

FOREWORD

This interim report describes work performed at the Columbus Aircraft Division of Rockwell International during the period from 1 June 1977 to 28 February 1978. This work was supported by the Office of Naval Research, under Contract N00014-77-C-0271. The Scientific Officer for the project was Dr. R. E. Whitehead. It is the first phase of an effort to develop a computer program for predicting the V/STOL performance of thrust augmenting ejector aircraft.

The results presented here owe much to the contributions of other members of the technical staff, in particular J. K. McCullough and J. H. DeHart. We would like to thank all of them for their valuable suggestions.

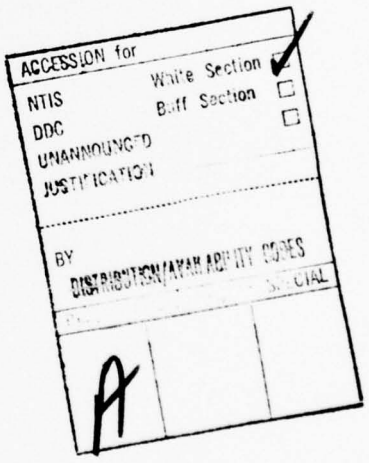

ABSTRACT

A method has been developed for calculating the static performance of thrust augmenting ejectors by matching a viscous solution for the flow through the ejector to an inviscid solution for the flow outside the ejector. In effect, the ejector shroud is considered to be "flying" in the secondary velocity field induced by the entrainment of the primary jets. A two-dimensional analysis utilizing a turbulence kinetic energy model for the inner, jet mixing solution and potential flow singularities for the outer, induced flow is described. This approach offers the advantage of including external influences on the flow through the ejector. Comparisons with data are presented for an ejector having a single central nozzle and Coanda jets on the walls. The accuracy of the matched solution is found to be especially sensitive to the jet flap effect of the flow just downstream of the ejector exit.

TABLE OF CONTENTS

LIST OF FIGURES

NOMENCLATURE

A	area
A_e	ejector exit area
A_{ij}	influence coefficients for V_v
a_{ij}	influence coefficient for u due to vortices
B_{ij}	influence coefficients for shroud source strengths
b_{ij}	influence coefficients for v due to vortices
c_{ij}	influence coefficients for u due to central jet and opposite wall jet
c_1	constant in turbulence model
c_2	constant in turbulence model
c_μ	constant in turbulence model
d_{ij}	influence coefficients for v due to central jet and opposite wall jet
F	shroud lift
G	rate of generation of turbulent kinetic energy
H	ratio of static pressure drop to the initial kinetic energy
J	thrust of wall jet at ejector exit
k	turbulence kinetic energy
ℓ_j	panel length of $j^{\underline{th}}$ source panel
m	number of source panels on ejector shroud
$\dot{m}_e$	rate at which mass flow is entrained
$\dot{m}_p$	primary mass flux
$\dot{m}_s$	secondary mass flux
M	mass flux ratio, $\dot{m}_s/\dot{m}_p$
n	number of discrete vortices
P	pressure
P_a	atmospheric pressure
P_e	pressure at ejector exit
ΔP	pressure drop with respect to ambient
q_j	sink strength per unit length on $j^{\underline{th}}$ panel
Q	sink strength
r	distance from singularity

r_w	coordinate normal to shroud leading edge
R	radius of jet curvature
R_w	radius of curvature of shroud leading edge
s	one half of sink panel length on ejector axis
T	actual thrust of primary flow
T_I	isentropic thrust of primary flow
u	velocity in the x-direction
u_J	Coanda jet velocity
u_o	initial primary flow velocity
U_m	mixed flow velocity outside ejector
U_p	primary flow velocity outside ejector
U_m^*	mixed flow velocity inside ejector
U_p^*	primary flow velocity inside ejector before mixing
U_s^*	secondary flow velocity inside ejector before mixing
v	velocity in the y-direction
V	magnitude of velocity induced by singularity distribution
V_e	entrainment velocity
V_s	velocity normal to a panel induced by the jets
V_v	velocity normal to a panel induced by vortices
x	coordinate in the direction of the ejector centerline
y	coordinate normal to the ejector centerline
α	angle of panel with respect to x-axis
γ	vortex strength per unit length
Γ	vortex strength
δ	wall jet thickness
ε	rate of dissipation of turbulence kinetic energy
θ_{ij}	angle between the normals to panels i and j
μ_t	turbulent viscosity
ξ	coordinate tangent to singularity panel
π	constant, 3.14159
ρ	fluid density
σ_k	constant in turbulence model
σ_ε	constant in turbulence model

τ	turbulent shear stress
T	thrust of the ejector
ϕ	augmentation ratio
ψ	stream function
ω	dimensionless stream function

INTRODUCTION

The U. S. Navy is developing several categories of V/STOL aircraft for use with smaller carriers, as a more economical means of maintaining sea control. Ejector thrust augmentation offers a solution to many of the problems that arise in the design of such V/STOL aircraft. A thrust augmenting ejector is a pneumatic device through which a large mass of air drawn from the atmosphere is pumped by the entrainment of a primary jet, as shown in Figure 1. The entrained air is accelerated by the turbulent mixing of the two streams within the ejector. By Newton's law of action and reaction, a force which is equal and opposite to the momentum change of the accelerated fluid is experienced by the ejector. Thus, significant increases in the thrust of turbojet and turbofan engines can be obtained by diverting the exhaust flow through an ejector pump.

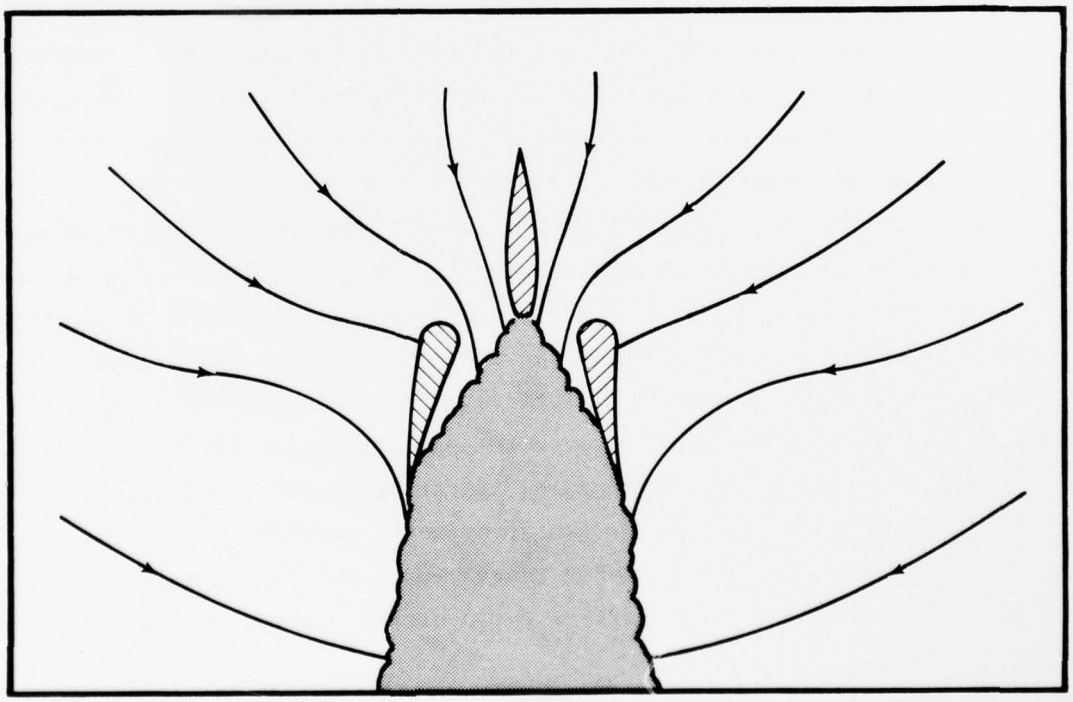

Figure 1. Entrainment by the Primary Jet Induces a Secondary Flow

Since ejectors can be designed to deflect as well as augment the engine thrust, they can be used to give an aircraft having a basic thrust to weight ratio less than one the direct jet lift necessary for vertical takeoffs and landings. In effect, the aircraft is given a variable bypass propulsion system: mass flow and thrust are augmented by passing the flow through an ejector for vertical flight, and reduced by exhausting the flow through a conventional nozzle for horizontal flight. When the ejector is integrated with the wing to produce a lift-propulsion system, separate reaction jets are not required for control during hover; control forces are generated by differential action of the ejectors. In addition, the ejector wing has good transition and STOL performance, because the exhaust flow acts like a jet flap to increase the circulation lift of the wing.

Although consideration of the ejector for aircraft thrust augmentation began more than thirty years ago,[1] development has been largely by experiment. However, analytic methods are necessary for conceptual studies and to reduce test requirements. In order to calculate ejector performance without solving the full Navier-Stokes equations, some approximations must be made. The analyses that have been developed are broadly based on von Karman's now classical approach,[2] which utilizes streamwise integration of the governing equations. If the ejector is relatively long and the diffuser angle is small, gradients of the normal stress and the variation of pressure across the flow can be neglected. This reduces the governing elliptic equations to a parabolic set which can be solved by marching through the ejector in the streamwise direction. The solution is obtained by iterating on the inlet velocity until the exhaust pressure matches the atmospheric pressure outside the ejector. A method incorporating a mixing length model for the turbulence was developed by Gilbert and Hill[3] for a simple ejector having a single

primary jet, while DeJoode and Patankar[4] employed a two-equation model for the turbulence in an ejector with hypermixing[5,6] and Coanda jets.

Even though the elliptic boundary value problem can thus be transformed to an initial value problem which is more easily solved, the basic elliptic character of the flow field is unchanged. This means that there are cases for which the classical momentum theories predict the wrong performance, or do not yield a solution, at all. For instance, as the walls of the ejector shroud are removed to infinity, the predicted augmentation ratio does not reduce to unity, as it must in the limit of an isolated turbulent jet. Also, when the ejector is short or the diffuser angle is large, the exhaust pressure is less than atmospheric pressure. This pressure difference is supported by the momentum of the exhaust jet, while the jet momentum depends in turn on the pressure difference. Thus, the exhaust pressure becomes a floating boundary condition, and a unique solution to the initial value problem cannot be obtained by classical methods.

The purpose of this paper is to present an ejector analysis not subject to these limitations. The primary elliptic effects are included by iterating between a parabolic solution for the flow through the ejector and an elliptic solution for the flow outside the ejector. This technique is similar to that used in coupling a solution for the displacement thickness of a wing boundary layer to a solution for the external flow. A parabolic solution for the turbulent mixing within the ejector was developed according to classical momentum theories. For the elliptical flow outside the ejector, a solution based on Bevilaqua's lifting surface theory[7] was developed. Briefly, the augmenting force is related to the lift on a wing, and the circulation is determined as a function of the jet entrainment.

A two-dimensional analysis utilizing a turbulence kinetic energy model for the inner, viscid solution and vortex lattice methods for the outer inviscid solution is described. Results are presented for an ejector having a single center nozzle and jets on the walls, but other configurations can be analyzed with the same approach. In the next section an outline of ejector theory is presented to introduce the mathematical models used in this analysis. The solution algorithms and the method of iteration are described in the following sections. The predictions of this new model are compared with classical solutions and experimental data in the final section.

PRINCIPLE OF THRUST AUGMENTATION

Circulation Thrust

Although ejector thrust augmentation may seem to utilize a new principle of lift generation, it actually involves no more than a novel application of the familiar circulation theorem of aerodynamic lift. An isolated jet induces an essentially lateral flow of entrained air, as sketched in Figure 2. However, the distributions of pressure and velocity in the flow entrained by the jet are altered by the presence of a shroud. A circulation which redirects the entrained flow through the ejector is generated around each of the shroud sections, as shown in Figure 3. The shroud can therefore be considered to be "flying" in the velocity field of the flow entrained by the jet, and it experiences a force analogous to the lift developed on a wing fixed in a moving stream.

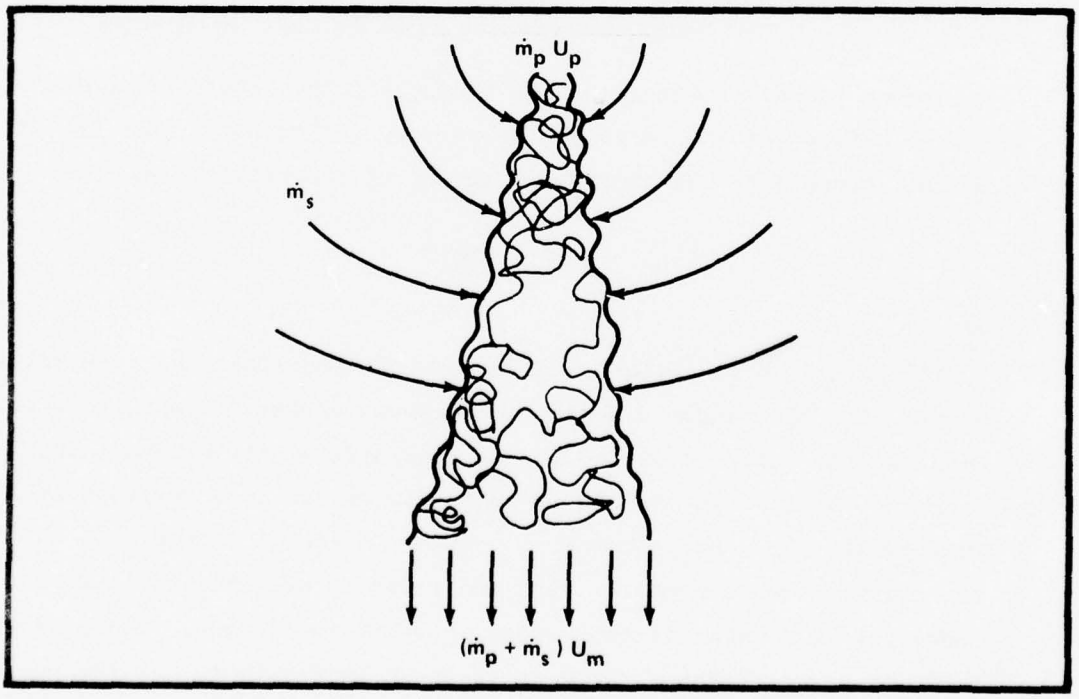

Figure 2. Streamlines of the Flow Induced by a Free Jet

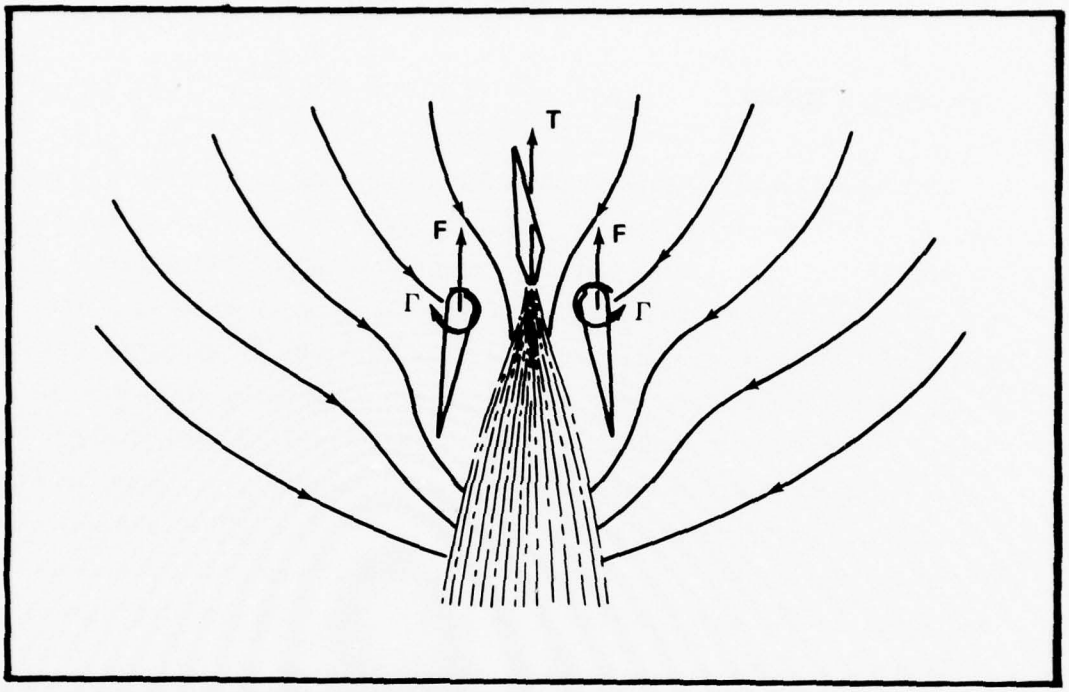

Figure 3. A Circulation Redirects the Flow through the Ejector

According to this lifting surface theory,[7] the thrust augmentation ϕ can be defined as the ratio of the primary jet thrust T plus the "lift" on the shroud F to the isentropic thrust of the primary mass T_I:

$$\phi = \frac{T + F}{T_I} \tag{1}$$

The thrust augmentation results from the fact that the interaction between the flow induced by the entrainment of the jet and the vorticity bound in the sections of the shroud generates a pair of equal and opposite forces. The origin of these forces can be understood by a consideration of the interaction between a sink of strength Q, which represents a section of the jet, and a vortex of strength Γ, which represents a segment of the vortex sheet in the shroud. These singularities are a distance r apart, as shown in Figure 4. At the vortex,

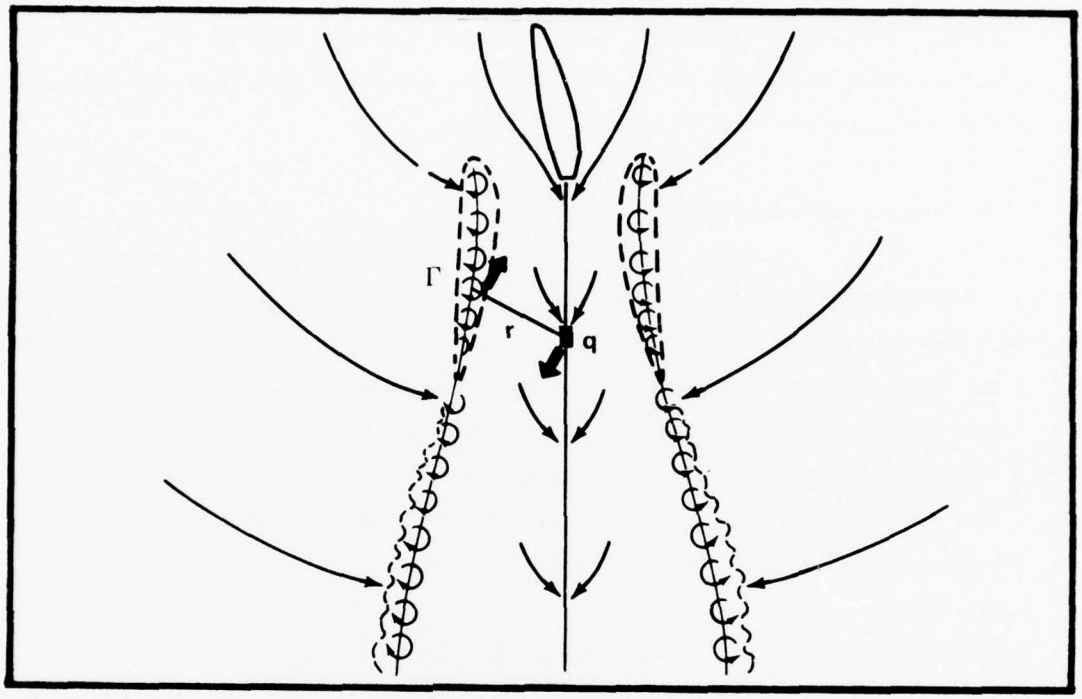

Figure 4. Mutually Induced Forces on a Sink-Vortex Pair

the sink induces a velocity of magnitude $Q/2\pi r$, directed along r. The vortex therefore experiences a force $\rho\Gamma Q/2\pi r$, perpendicular to r. At the sink, the vortex induces a velocity of magnitude $\Gamma/2\pi r$, perpendicular to r. The sink therefore experiences a force $\rho Q\Gamma/2\pi r$, also perpendicular to r, but opposite to the force on the vortex. The net effect of the interactions between all the sinks and vortices is a force which increases the thrust of the jet, and an equal but opposite reaction on the shroud.

The force on the shroud can be recognized as the vortex force given by the Kutta-Joukowski theorem for airfoil lift. This force appears in the pressure distribution on the surface of the shroud, primarily as a leading edge suction. However, the thrust on the jet sinks may not be as familiar. This force is conceptually similar to the ram drag that develops on an aircraft engine inlet, but it must be remembered that the

sink/vortex interaction, as described, is only valid in irrotational flows. The fluid entrained into the jet becomes rotational, so that an understanding of how this force actually developes requires consideration of the jet mixing process.

Jet Thrust Augmentation

The mixing process is basically an inelastic collision between the jet and the surrounding fluid. As such, jet mixing is governed by the same laws of momentum and energy conservation as simple collisions between discrete particles. In free jet mixing, the momentum flux is conserved and there is a corresponding loss of kinetic energy to turbulence and heat. However, the circulation accelerates the entrained flow entering the ejector and, according to Bernoulli's equation, the pressure drops. Inside the ejector, before mixing, the velocities in the primary and secondary flows are given approximately by

$$U_P^* = \left(U_p^2 + \frac{2\Delta P}{\rho}\right)^{1/2} \tag{2}$$

$$U_S^* = \left(\frac{2\Delta P}{\rho}\right)^{1/2} \tag{3}$$

in which ΔP is the pressure drop induced by the circulation. Momentum is conserved during the mixing process itself, so that

$$\dot{m}_P U_P^* + \dot{m}_S U_S^* = (\dot{m}_P + \dot{m}_S) U_m^* \tag{4}$$

The mixed stream decelerates as it leaves the low pressure region, and its final velocity is

$$U_m = \left(U_m^{*2} - \frac{2\Delta P}{\rho}\right)^{1/2} \tag{5}$$

The ratio of the final momentum, $(\dot{m}_P + \dot{m}_S)U_m$, to the initial momentum, $\dot{m}_P U_P$, may be evaluated by substituting in turn for U_m, then U_m^*, and

finally for U_p^* and U_S^*. Performing the substitutions yields for this ratio

$$\phi = \sqrt{1 + 2M \left(H^2 + H\right)^{1/2} - H} \qquad (6)$$

in which M is the mass flux ratio, $M = \dot{m}_S/\dot{m}_p$, and H is the ratio of the static pressure drop to the initial kinetic energy, $H = \Delta P/1/2\rho U_p^2$.

If the pressure drop is negligibly small, $H \ll 1$ and the solution reduces to the case of free jet mixing. Momentum is conserved, $\phi = 1$. On the other hand if the pressure drop is relatively large, $H \gg 1$ and the momentum ratio simplifies to

$$\phi = (1 + M)^{1/2} \qquad (7)$$

so that the thrust increases with the entrainment ratio. The dependence of ϕ on intermediate values of H is sketched in Figure 5.

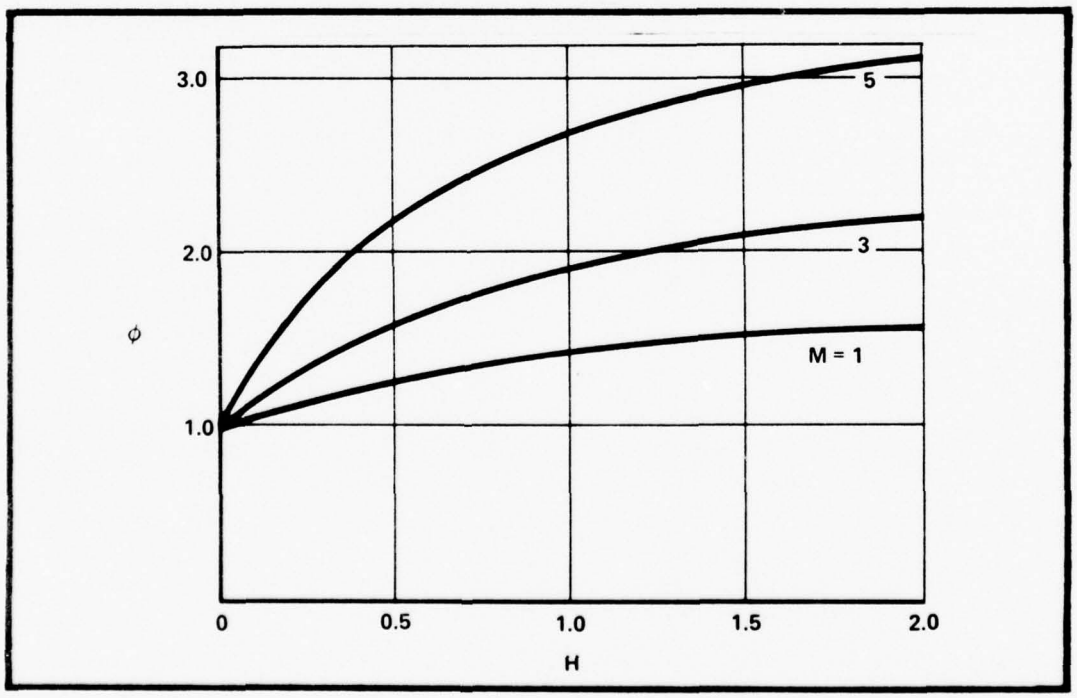

Figure 5. Jet Thrust Augmentation as a Function of Entrainment and Pressure Drop

Thus, ejector thrust augmentation is generated by the turbulent mixing of the primary jet and secondary stream in a region of reduced pressure. The increase in thrust that results when the mixed flow returns to ambient pressure appears as a reaction force on the ejector shroud. Although these forces are related to the mutually induced forces on a vortex and sink in irrotational flow, the flow through the ejector actually includes regions of interacting irrotational and turbulent fluid, subject to lateral straining, and streamwise curvature, with variations of temperature and density. In the following section a method of calculating these forces in a real fluid will be developed from the principles outlined in this section.

INVISCID, OUTER SOLUTION

Jet Sink Distribution

The Navier-Stokes equations for steady fluid motion are elliptic, which means that the domain of influence of a point disturbance is the entire flow volume. That is, pressure and stress gradients transmit the effect of local disturbances to every other point in the flow; thus, the flow through the ejector depends on boundary conditions outside the ejector as well as within the shroud. The basis of the present analysis is the separation of the flow field into two regions: the region of viscous mixing within the ejector and the inviscid region around it. Significant elliptic effects are transmitted through the pressure field of the external flow, while the turbulent mixing is accurately calculated for the internal flow. Short of solving the full Navier-Stokes equations, matching the solutions in these regions is the only way to predict ejector performance. Since it reduces the requirements for computer time and storage, the matching procedure has some advantage over the full solution.

The circulation generated around each section of the ejector shroud will be calculated by solving a system of equations which specify that the shroud must be a streamline of the flow induced by the entrainment of the jets. For this calculation, the strengths of the sinks which represent each jet are considered to be known. These strengths are determined from the turbulent mixing of the jets computed in the viscous solution during the previous iteration.

The entrainment of the central jet is represented by a series of overlapping, triangular sink distributions on the axis of the ejector, as shown in Figure 6. Each distribution is identified by the index of its central point, where the strength of the sink is q_j; every panel is

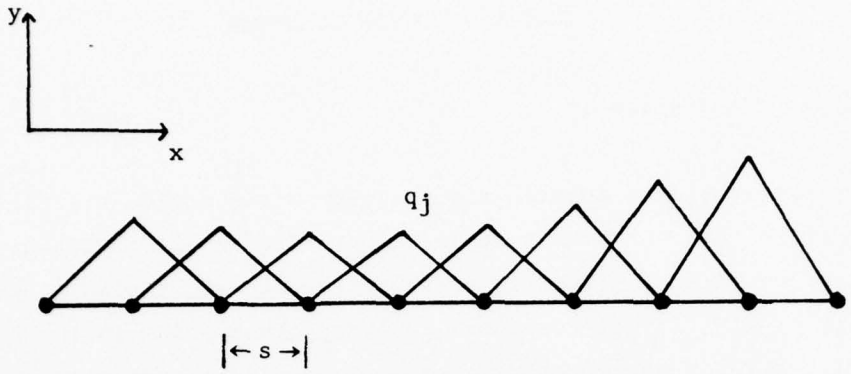

Figure 6. Triangular Sink Panels on the Axis of the Ejector

the same length, 2s. In incompressible flow, the horizontal and vertical components of velocity induced at an arbitrary point P(x, y) by such a distribution are given by:

$$u(x,y) = q_j \int_j \frac{x-\xi}{2\pi r^2} \left(1 \pm \frac{\xi}{s}\right) d\xi \qquad (8)$$

$$v(x,y) = q_j \int_j \frac{y}{2\pi r^2} \left(1 \pm \frac{\xi}{s}\right) d\xi \qquad (9)$$

in which ξ is a coordinate on the path of integration over the panel, and r is the distance $\left[(x-\xi)^2 + y^2\right]^{1/2}$. The plus sign (+) is used for the rising side of the triangle, from -s to the center, and the minus sign (-) for the falling side, from the center to +s. The integration of these expressions is given in Appendix I.

The surface of the ejector shroud is represented by m source panels of different lengths, ℓ_j, and uniform strength, q_j, as shown in Figure 7. Because a single sheet of sinks cannot provide the jump in entrainment necessary to model the presence of a wall jet on the inner surface of the shroud only, both the inner and outer surfaces must be represented by source/sink panels. The horizontal and vertical components of velocity induced at an arbitrary point by a uniform source distribution are given by:

$$u(x,y) = q_j \int_j \frac{y}{2\pi r^2} \, d\xi \tag{10}$$

$$v(x,y) = q_j \int_j \frac{x - \xi}{2\pi r^2} \, d\xi \tag{11}$$

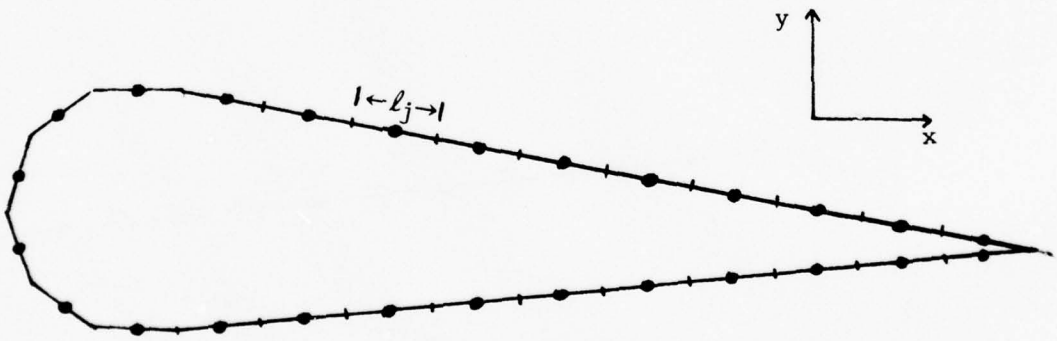

Figure 7. Uniform Source/Sink Panels on the Surface of the Shroud

These expressions are also integrated in Appendix I. The velocity components induced at each point in the flow are obtained by adding up the contributions of every panel.

Shroud Vorticity Distribution

A vortex lattice method was used to determine the circulation density of the shroud. The continuous vorticity distribution is replaced by n discrete vortices of strength Γ_j, located at x_j, the quarter chord of the panels shown in Figure 8. It was found that better results were obtained if the vortex sheet is placed on the inner surface of the shroud, rather than on the mean camber line. All the flow singularities which represent the shroud geometry and jet effects must induce the known entrainment (inflow) velocities on the surface of the shroud. However, the source/sink distribution on each surface already satisfies this boundary condition. Therefore, the resultant of the velocities induced by all the other singularities must be tangent to the inner

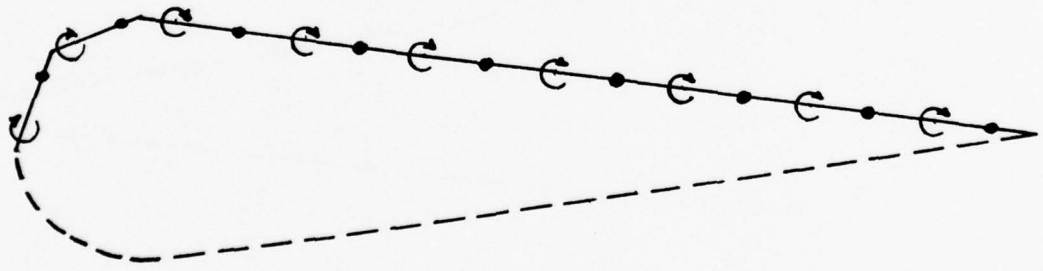

Figure 8. Discrete Vortex Lattice on the Inner Surface of the Shroud

surface of the shroud; that is, the normal velocity induced by the vortex sheet must be equal but opposite to the normal velocity induced by the central jet and opposite wall jet.

The vortex strengths are determined by satisfying this boundary condition at n points which correspond to the three quarter chord station on each panel. In calculating the velocity induced by the vortex sheets, it is convenient to simultaneously consider the influence of each vortex and its image on the opposite side of the ejector. The horizontal and vertical components of velocity induced at a point $P(x_i, y_i)$ by the vortex pair of strength Γ_j at the points $P(x_j, y_j)$ and $P(x_j, -y_j)$ are

$$u(x_i, y_i) = \left(\frac{y_j - y_i}{2\pi r_{ij}^2} - \frac{y_j + y_i}{2\pi r_{i,-j}^2} \right) \Gamma_j \tag{12}$$

$$v(x_i, y_i) = \left(\frac{x_j - x_i}{2\pi r_{ij}^2} + \frac{x_j - x_i}{2\pi r_{i,-j}^2} \right) \Gamma_j \tag{13}$$

in which $r_{ij} = \left[(x_i - x_j)^2 + (y_i - y_j)^2 \right]^{1/2}$ is the distance between points. Thus, the contribution to the velocity normal to panel-i by both vortex sheets is

$$V_v = \sum_j (b_{ij} \cos \alpha_i - a_{ij} \sin \alpha_i) \Gamma_j \tag{14}$$

in which the influence coefficients, a_{ij} and b_{ij}, have the form given in Equations (12) and (13), and α_i is the angle of panel-i relative to the ejector axis. Similarly, the normal velocity induced by the central jet and the opposite wall jet is

$$V_s = \sum_j (d_{ij} \cos \alpha_i - c_{ij} \sin \alpha_i) q_j \tag{15}$$

in which the range of the index j is over both jets, so that the influence coefficients are given by Equations (8) and (9) or Equations (10) and (11), as appropriate. As previously noted, the sink strengths are known, having been determined by the solution of the turbulent mixing problem in the previous iteration.

Since the resultant of the normal velocities induced by the jet and vortex sheet must be zero, V_v is set equal but opposite to V_s at each control point,

$$-V_{s_i} = A_{ij}\ \Gamma_j \tag{16}$$

The summation convention for repeated indices is intended to apply. Thus, this expression represents a set of simultaneous algebraic equations for the Γ_j. The influence coefficients, A_{ij}, have the form given in Equation (14). This equation was solved for the Γ_j by triangularization of the coefficient matrix.

VISCOUS, INNER SOLUTION

Governing Equations

The entrainment which represents the effect of the jets is calculated from a solution for the turbulent mixing within the ejector. It is possible to calculate the rate of entrainment without solving the complete three-dimensional mixing problem, by taking advantage of the flow geometry. Since there is a primary direction of flow (through the ejector) it is assumed that the thin shear layer approximation can be applied. This reduces the governing elliptic equations to a parabolic set. The effect of a disturbance is confined to regions downstream of the disturbance, and so the equations can be solved by marching through the ejector in the streamwise direction. This results in considerable savings in computer storage and time compared to a solution of the elliptic mixing problem.

The two-dimensional flow in an ejector cross section is governed by the continuity equation and the streamwise momentum equation. The thin shear layer approximation means that the gradients of the normal stress are negligible, and the pressure P is constant in each plane normal to the direction of flow. Thus, only shear stresses caused by velocity gradients across the flow are significant. An additional assumption that the fluid density ρ is uniform was also made. Under these assumptions, the equation for the conservation of mass and momentum through the ejector become:

$$\text{Continuity:} \quad \rho \frac{\partial u}{\partial x} = 0 \tag{17}$$

$$\text{Momentum:} \quad \rho u \frac{\partial u}{\partial x} = \frac{\partial \tau}{\partial y} - \frac{dP}{dx} \tag{18}$$

Here, u is the time averaged velocity in the streamwise direction, and τ is the turbulent shear stress. Laminar stresses are assumed to be negligible.

In order to provide accurate calculations of the turbulent stresses in each region of the flow (initial and developed sections of the free jet, inner and outer layers of the wall jet, and the merged region) the advanced two equation turbulence model of Launder and Spalding[8] was used for turbulence closure. This model employs differential equations for the turbulence kinetic energy and its rate of dissipation; the eddy viscosity at each point is calculated from these quantities. This approach has previously been used in more complex jet flows by DeJoode and Patankar,[4] where it yielded satisfactory results.

According to the usual eddy viscosity assumption, the turbulent stress is first expressed in terms of a turbulent viscosity μ_t and the velocity gradient in the cross stream direction:

$$\tau = \mu_t \frac{\partial u}{\partial y} . \tag{19}$$

The two-equation turbulence model developed by Launder and Spalding[8] gives the turbulent viscosity in terms of two parameters, for which two differential equations are solved. The expression for turbulent viscosity is:

$$\mu_t = \frac{c_\mu \rho k^2}{\epsilon} \tag{20}$$

where c_μ is a constant, k is the kinetic energy of turbulence, and ϵ is the rate of its dissipation. In two-dimensional parabolic flows, the governing equations for k and ϵ are:

$$\rho u \frac{\partial k}{\partial x} = \frac{\partial}{\partial y}\left(\frac{\mu_t}{\sigma_k} \frac{\partial k}{\partial y}\right) + G - \rho \epsilon \tag{21}$$

$$\rho u \frac{\partial \epsilon}{\partial x} = \frac{\partial}{\partial y}\left(\frac{\mu_t}{\sigma_\epsilon} \frac{\partial \epsilon}{\partial y}\right) + (c_1 G - c_2 \rho \epsilon) \frac{\epsilon}{k} \tag{22}$$

The quantity G is the rate of generation of k by the action of the velocity gradient and is expressed as:

$$G = \mu_t \left(\frac{\partial u}{\partial y} \right)^2 \tag{23}$$

This turbulence model involves five empirical constants. According to the recommendation of Launder and Spalding[8] the following values of the constants are appropriate for ordinary jets:

c_μ	c_1	c_2	σ_k	σ_ϵ
0.09	1.44	1.92	1.0	1.3

The effect of hypermixing[5,6] can be simulated by increasing the value of c_μ by a factor of 5 to 6 in the central jet.

Method of Solution

The procedure used to solve the governing equations is very similar to the method devised by Patankar and Spalding.[9] The equations are transformed from a Cartesian coordinate system (x,y) to a (x,ω) system where ω is a dimensionless stream function defined as:

$$\omega = \frac{\psi}{\psi_{total}} \tag{24}$$

where $d\psi \equiv \rho u dy$ and ψ_{total} is the total mass flow rate in the computational domain. The method employs a finite-difference marching procedure; from known conditions at an upstream cross section, x, the flow field at the downstream cross section, $x + \Delta x$, is computed. This marching process is continued until the domain of interest is covered. The initial conditions are determined from the velocities induced in the ejector inlet by the vorticity distribution obtained in the outer solution on the previous iteration. The finite-difference equations are formed by integrating the differential equations over a small control volume surrounding each grid point. The resulting non-linear

equations are linearized by using upstream values of the flow variables to evaluate coefficients involving cross stream convection and diffusion. The equations are solved by the use of the tri-diagonal matrix algorithm.

The procedure employed for evaluation of the unknown pressure gradient that appears in the momentum equation requires special mention. A technique developed by Sparrow, et al[10] is used to determine the correct value of dP/dx. Briefly, a non-linear equation for dP/dx is derived by combining the momentum equation with the constraint that the value of dP/dx must result in values of u which satisfy the requirements of continuity. This equation is solved by an iteration algorithm that is an adaptation of the Newton-Raphson procedure. The convergence is fast and the procedure eliminates the arbitrariness and the resultant inaccuracy of the technique originally developed by Patankar and Spalding.[9]

Jet Entrainment Rate

The jet entrainment is derived from the solution for the turbulent mixing within the ejector. In principle, the entrainment can be obtained by integrating the jet velocity profiles, and finding the difference in mass flux between successive stations. However, practical difficulties in defining the jet boundaries introduce considerable error in calculating the mass flux, and this procedure cannot be used at all beyond the point where the jets merge. For these reasons a method was developed for determining the entrainment indirectly, from the pressure rise within the ejector.

The connection between the entrainment rate and the pressure rise is illustrated in Figure 9, which shows the spreading of a single jet in a straight duct. As the jet spreads, fluid is entrained into the primary stream and the velocity of the secondary stream is correspondingly

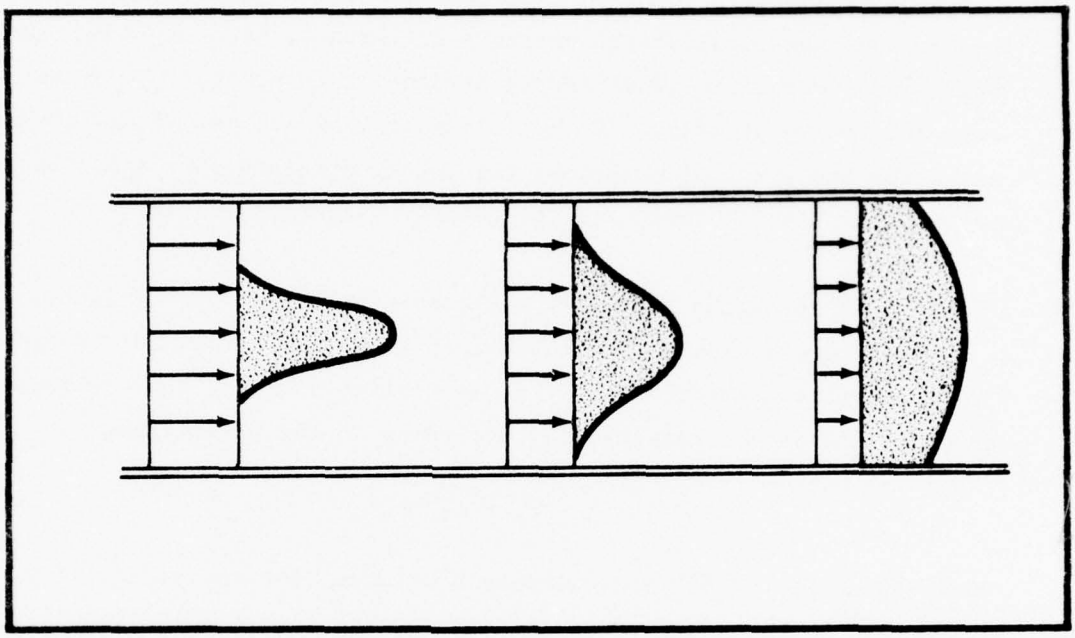

Figure 9. Spreading of a Turbulent Jet in a Duct

reduced. According to Bernoulli's equation, the static pressure in the secondary stream rises. The boundary of the jet continuously adjusts to equalize the pressure across the duct while providing the necessary entrainment. Mixing continues downstream of the point where the jet has spread to the walls, and the pressure rises accordingly. The static pressure can be related to an equivalent secondary velocity in this region. This velocity is shown in Figure 9.

The entrainment of the jet between two successive stations can therefore be calculated as the quantity of fluid that must be removed from the secondary stream to produce the observed pressure rise:

$$\dot{m}_e = \rho(2\Delta P_{i-1}/\rho)^{1/2} A_{i-1} - \rho(2\Delta P_i/\rho)^{1/2} A_i \qquad (25)$$

in which Bernoulli's equation is used to express the secondary velocity in terms of the local static pressure difference, $\Delta P_i = P_a - P_i$. For the general case, the cross sectional area of the duct, A_i, may vary from station to station. If there is more than one jet within the duct, as in the present configuration, the total entrainment is apportioned between the jets according to the relative spreading rates.

The sink strengths that will represent the effect of the jets in the inviscid calculation are determined from the entrainment of each jet. An entrainment velocity, V_e, is derived from the mass entrained between successive stations, $\dot{m}_e$, according to the definition,

$$V_e = \dot{m}_e / \rho \Delta x \qquad (26)$$

in which Δx is the distance between stations. For the central jet, the strengths of the q_j are determined by setting the velocity induced at the midpoint of each triangular distribution equal to the entrainment velocity at that point. *It is shown in Appendix II that* $q_j = -2V_e$ *at* each control point.

The strengths of the q_j for the wall jets on the surface of the ejector shroud are determined by simultaneously satisfying the known entrainment (inflow) boundary condition due to the wall jet on the inner surface of the shroud, and the condition of zero flow through the outer surface. By a transformation of coordinates, Equations (10) and (11) are used to calculate the normal component of velocity, V, induced by the j-th source distribution at the midpoint of the i-th panel. In Appendix II, the velocity induced at the midpoint of panel-i by the source distribution on panel-i is shown to be $V_i = q_i/2$. The contribution of every panel, including panel-i, is added at each control point. The normal velocity component at each control point is given by the summation,

$$V_i = \sum_j (v_{ij} \cos \theta_{ij} - u_{ij} \sin \theta_{ij})$$

in which θ_{ij} is the angle between the normals to panels i and j.

The induced velocity is set equal to the required entrainment velocity V_e at each control point, yielding a set of m simultaneous algebraic equations for the q_j,

$$V_{e_i} = B_{ij}\, q_j$$

in which the influence coefficients give the velocity induced at the point i by a source of unit strength on panel j. This matrix equation is solved for the q_j by triangularization of the coefficient matrix, B_{ij}. The solution yields sinks (negative sources) on the inner surface of the shroud and positive sources on the outer surface of the shroud.

Since the reaction to the thrust of the mixed stream appears in the pressure distribution on the surface of the shroud, the whole effect of the turbulent mixing is represented by the strength of these sinks. The velocities induced by the sinks determine the strength of the vortex sheet and the pressures on the shroud. Conversely, the requirement that the total vorticity must satisfy the Kutta condition determines the rate of entrainment by controlling the initial velocity of the secondary stream. The actual strength of the sinks and the magnitude of the circulation are determined by iteration between the turbulent and inviscid solutions, as described in the next section.

SOLUTION MATCHING PROCEDURE

Method of Iteration

The inner and outer routines are incorporated into a single computer program which yields a matched solution by iterating between the rate of entrainment by the jets and the circulation around the shroud. For a simple ejector having a single primary jet, the method of iteration is relatively straightforward. The sequence is outlined in the following:

1. An assumption is made for the magnitude of the secondary velocity at the inlet of the ejector.

2. The entrainment of the jet is computed from this initial condition by marching through the ejector with the turbulent mixing routine.

3. The equivalent sink strengths within the ejector are calculated from the pressure gradient. Downstream of the ejector exit, it is specified that the sink strengths decay as in a free jet; that is, as $x^{-1/2}$.

4. The vorticity distribution is computed with the inviscid routine, by requiring that the shroud be a streamline of the flow induced by the sink distribution.

5. The velocity induced at the ejector inlet by all the sinks and vortices is calculated and compared to the initial guess.

If these agree, the solutions are matched. Otherwise, steps 2 through 5 are repeated until convergence is achieved, or the routines break down due, for example, to flow separation from the inner surfaces of the shroud.

Since such ejector configurations separate at typically low inlet and diffuser area ratios, without producing significant augmentation, these are of limited interest. When wall jets are added to prevent separation, the maximum augmentation increases, but a new flow phenomenom complicates

the calculation procedure. Curvature of the jet sheet leaving the trailing edge of the flap, as shown in Figure 10, supports a low pressure region behind the ejector. Morel and Lissaman[11] pointed out the similarity of this action to that of the jet flap, and described the phenomenon as a "jet flap diffuser."

Because the pressure difference is supported by the momentum of the exhaust jet, while the jet momentum depends in turn on the pressures at the ejector exit, another calculation is required to determine the influence of the jet flap diffuser. This influence was determined using an approach developed from the classical jet flap theory of Spence.[12] The pressure difference across the trailing jet sheet is related to the strength of an equivalent vortex sheet,

$$\rho u \gamma = \Delta P \tag{29}$$

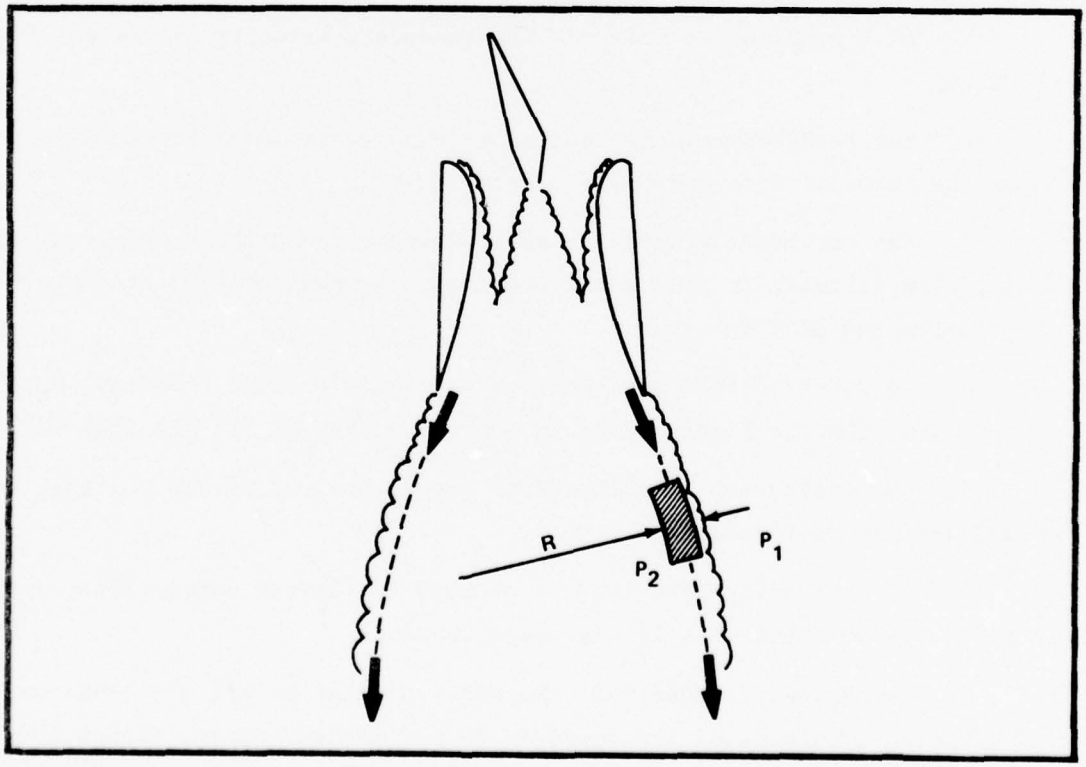

Figure 10. Curvature of the Trailing Jet Balances the Pressure Difference

so that the basic mathematical problem becomes finding a vorticity distribution which makes the jet sheet a streamline of the flow. Since the pressure difference is balanced by inertia forces due to curvature of the jet sheet, as shown in Figure 10, the radius of jet curvature, R, is given by

$$\frac{J}{R} = \Delta P \tag{30}$$

in which J is the thrust of the wall jet at the ejector exit. To a first approximation, both the jet thrust and radius of curvature can be assumed constant.

These two additional boundary conditions for the shape and strength of the jet flap diffuser are satisfied as part of the iteration to match the inner and outer solutions. The calculation sequence in this case is similar to that outlined previously:

1. An assumption is made for the secondary velocity at the ejector inlet.

2. The turbulent mixing routine is used to compute the development of the internal flow up to the ejector exit.

3. The curvature of the jet sheet which defines the boundary of the jet flap diffuser is calculated according to Equation (30) from the exit pressure and wall jet thrust.

4. Considering this jet sheet to represent a solid boundary, computation of the turbulent mixing is continued through the jet flap diffuser.

5. The equivalent sink strengths are determined within the ejector and jet flap diffuser.

6. The vorticity distribution on both the shroud and jet flap diffuser are computed with the inviscid routine.

7. The velocity induced at the ejector inlet by all the sinks and vortices is calculated and compared to the initial guess. Steps 2 through 7 are repeated until these agree.

In this calculation the length of the jet flap diffuser is defined to be the point where the jet sheets become parallel to each other and the axis of the ejector. When the iteration converges and the solutions are matched, the pressure within the ejector reaches atmospheric pressure at this point. In effect, the Kutta condition for the vorticity distribution is satisfied at the end of the jet flap diffuser, rather than at the trailing edge of the ejector shroud. In general, this approximation gives good results. However, if the jets do not merge until far downstream of the ejector exit, Marsters[13] has observed that the jets can curve back toward the axis and the pressures within the jet flap diffuser can actually rise above atmospheric pressure. Further development of the method will be required in order to obtain a solution in such cases.

Evaluation of the Thrust Augmentation

The thrust of the ejector is equal to the sum of the initial jet thrust plus the force on the shroud. In principle, it can be evaluated either by integrating the thrust of the mixed flow at the ejector exit, or by finding the resultant of the pressure and shear stresses on the surface of the shroud. In practice, integrating the stream thrust is relatively easy to do, while a large number of panels and an additional calculation of the skin friction are required to evaluate the force on shroud. However, because the pressure distribution is needed to estimate surface loads and hinge moments, both calculations are performed.

The stream thrust is evaluated at the exit of the ejector. Although any station in the jet wake should give the same result, the somewhat artificial treatment of the flow in the jet flap diffuser led to selection of the exit plane for this calculation. The thrust of the ejector is given by

$$\tau = \int_{A_e} \rho u^2 dy - (P_a - P_e)A_e \qquad (31)$$

in which P_e and A_e are the static pressure and area at the exit. Because the flow velocities are constant over a small control volume surrounding each grid point, integration of the stream thrust involves a simple summation of the thrust increment from each control volume. The static pressure is constant across the exit. It should be noted that even though the pressure force is negative, lowering the exhaust pressure, as with the jet flap diffuser, results in a net thrust increase. This is because the momentum flux is increased more than the pressure force is reduced.

The surface pressure distribution is determined from the tangential velocities induced at the surface of each panel. Actually, these pressures are more representative of the pressures at the outer edge of the wall jets. The high curvature of the wall jets over the leading edge of the shroud induces a significant radial pressure gradient across the jet. The resulting decrease in pressure at the surface is given by

$$dP = - \int_0^{\delta} \frac{\rho u_J^2}{R_w} \, dr_w \qquad (32)$$

in which $\rho u_J^2 / R_w$ is the inertia force which resists the turning of the jet, and δ is the jet thickness. This contribution to the surface pressure has not been included in the present analysis.

RESULTS AND DISCUSSION

Comparison with Experiment

In order to evaluate the basic lifting surface theory that the force on the shroud is related to the lift on a wing, the prediction of this analysis will be compared to experimental data. There are no exact solutions for the surface pressures or thrust augmentation; however, comparisons will be made with the results of classical analyses to determine if the primary elliptic effects have been correctly predicted. A sketch of the test ejector is shown in Figure 11. It combines a single central nozzle with Coanda jets on the inner surface of the shroud. A slot in each endwall at the ejector throat provides a boundary layer control jet to prevent separation of the flow from these surfaces. In this configuration, 60% of the primary flow is in the central jet, 17% goes to each of the Coanda jets, and the remaining

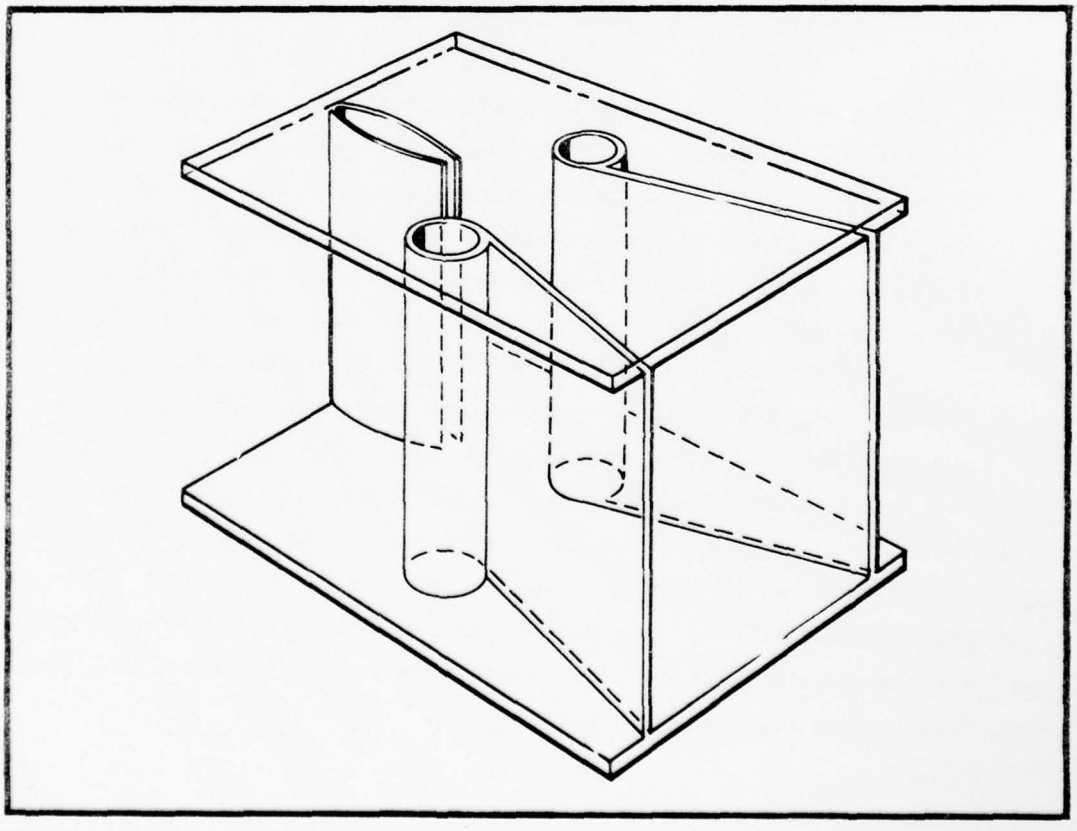

Figure 11. Sketch of the Experimental Ejector

6% of the primary flow is divided between the two endwall jets. The ejector has a span of 36 cm, a length of 27 cm, and has a throat 12 cm wide. The inlet area ratio is approximately 11.

The test ejector is supported on four flexible rods which are attached to a supporting frame. The net thrust is measured with two load cells installed on connecting arms between the frame and ejector. High pressure air is supplied to the primary jets from a single source, but the rate of flow to each nozzle is measured separately, with a calibrated venturi in each of the feed lines. Internal screens and baffles are used to smooth out spanwise variations in the jet velocity, so that the stagnation pressure is measured with a total pressure probe in the exit of each nozzle. The isentropic reference thrust is calculated as the product of the measured primary mass flow and the velocity defined by an isentropic expansion from the measured stagnation pressure to atmospheric pressure. It is estimated that the error in these measurements is within $\pm 3\%$ of the mean.

In Figure 12 the calculated change in the thrust augmentation ratio with the diffuser area ratio is compared to experimental values. At low diffuser area ratios the thrust augmentation is underpredicted by approximately 6%, while good predictions of the maximum augmentation are obtained. This result is a consequence of the approach taken in calculating the jet flap effect. Because the length of the jet flap diffuser is defined by the point where the jet sheets become parallel, the jet diffuser length goes to zero as the diffuser angle of the duct is reduced. Most of the discrepancy at the low diffuser area ratios can probably be attributed to this effect. With this perspective, the agreement between analysis and experiment can be judged satisfactory. It should be noted that a plane slot nozzle was installed in the test ejector to provide a simple, two-dimensional jet for these comparisons. The augmentation can be significantly increased by installing a hypermixing or multi-lobe nozzle.

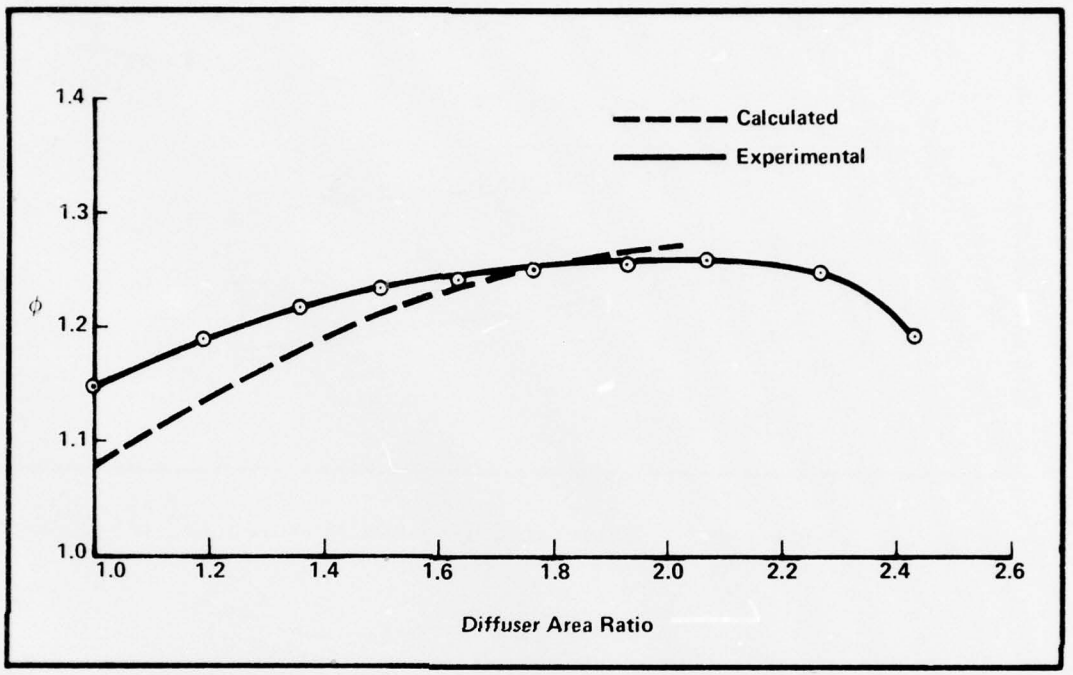

Figure 12. Comparison of the Effect of Calculated and Experimental Changes in the Diffuser Area Ratio

The calculated jet boundaries are compared with the measured boundaries in Figure 13. Since the turbulence constants were not adjusted for this case, but derived from other flows, the agreement is particularly good. The predictions of the shape and length of the jet flap diffuser are also satisfactory. In Figure 14 the calculated velocity distributions at three stations within the ejector are compared. The profiles from the inner, viscous solution show the spreading of the jets, as well as the reduction in secondary velocities. Because the diffuser walls are diverging in this case, not all the change in secondary velocity is due to entrainment; both the jet and secondary stream decelerate as a result of the change in cross sectional area.

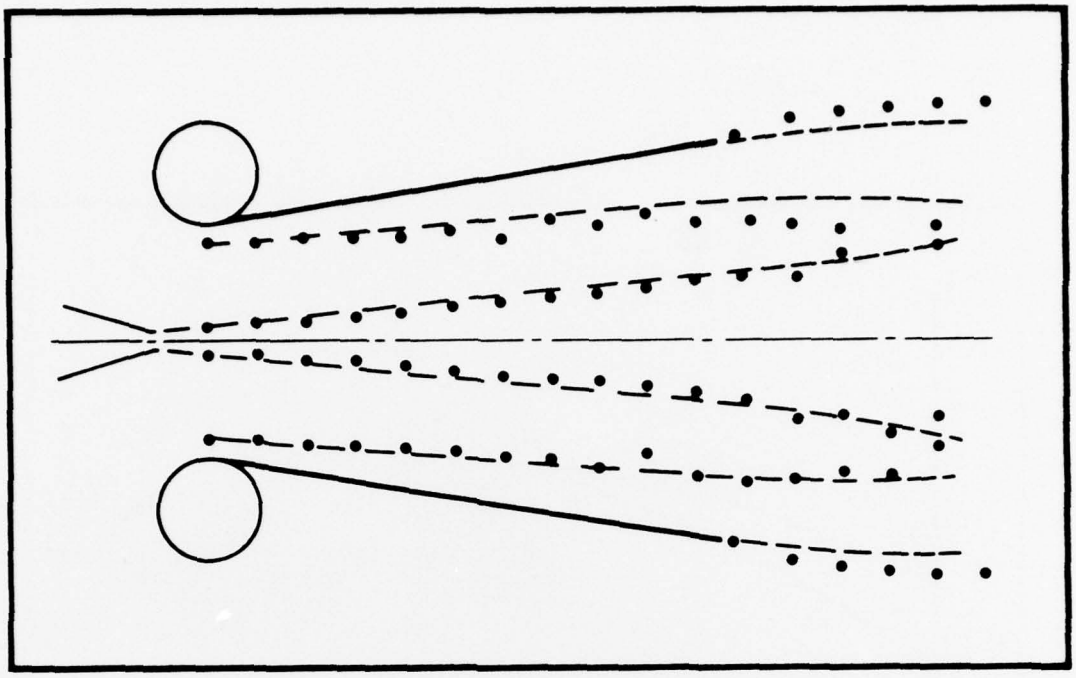

Figure 13. Comparison of Calculated (--) and Measured (•) Jet Spreading Rates

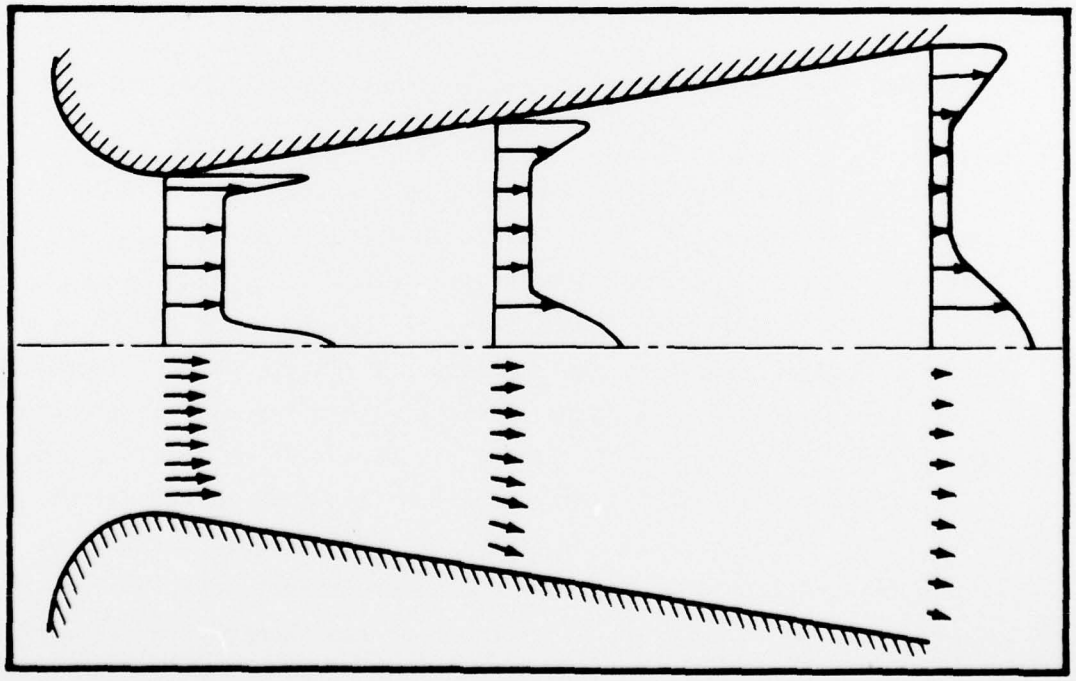

Figure 14. Comparison of Velocity Distributions Calculated by Viscous and Inviscid Solutions

Due to the assumption that the static pressures are constant at each axial station, the secondary velocities in the viscous solution are uniform; further, there is no transverse velocity component. The inviscid velocity distributions, shown on the other side of the ejector, indicate the extent of the actual skewness and the magnitude of the transverse velocities. Since the jets are replaced by equivalent sinks in the inviscid solution, the jet profiles are not seen in this case. The secondary velocities are generally uniform within the diffuser section. However, the effect of the high inlet curvature reduces the secondary mass flow through the ejector: since the inlet pressures are matched, the speed of the inlet flow is the same in each solution, but the inclination of the inviscid velocity vectors produces a "tilt loss" in axial mass flow. Curvature effects can be added to the viscous solution, and this will provide a better match of the mass flows. The predicted pressure rise through the ejector and the sink strengths derived from it are shown in Figure 15.

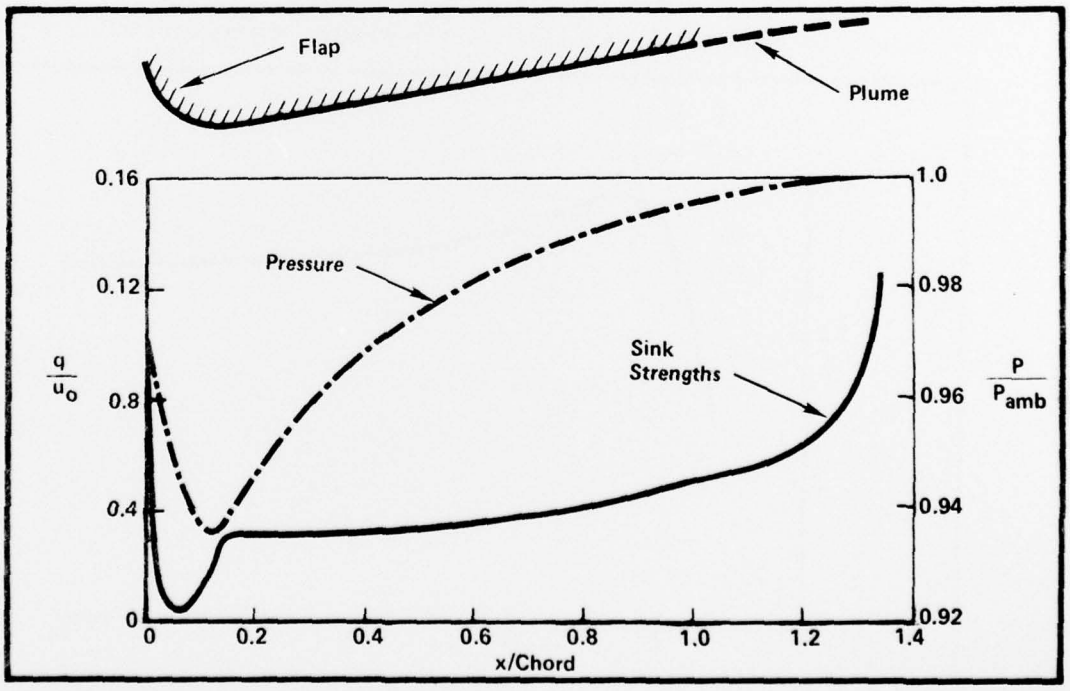

Figure 15. Predicted Static Pressure Gradient and Equivalent Sink Strengths

Prediction of Elliptic Effects

According to classical momentum theories,[2,3,4] the thrust augmentation ratio increases monotonically with ejector inlet area ratio. In the limit of very large inlet area ratios, the augmentation approaches $\phi = 2.0$, with no diffusion. With diffusion, correspondingly larger values of augmentation are predicted. This is because the parabolic flow assumption constrains the secondary flow to be always parallel to the ejector axis. The lifting surface theory[7] correctly predicts that the augmentation ratio approaches unity in this limit, as it must for an isolated turbulent jet. But, as the inlet area ratio approaches unity in the opposite limit, an unrealistic increase in the augmentation is predicted. This is because the effect of the circulation velocities in reducing the rate of entrainment are neglected.

Because it represents a merging of these two theories, the present interaction analysis has the correct behavior in both limits. Figure 16 shows the predicted variation of the thrust augmentation ratio as a

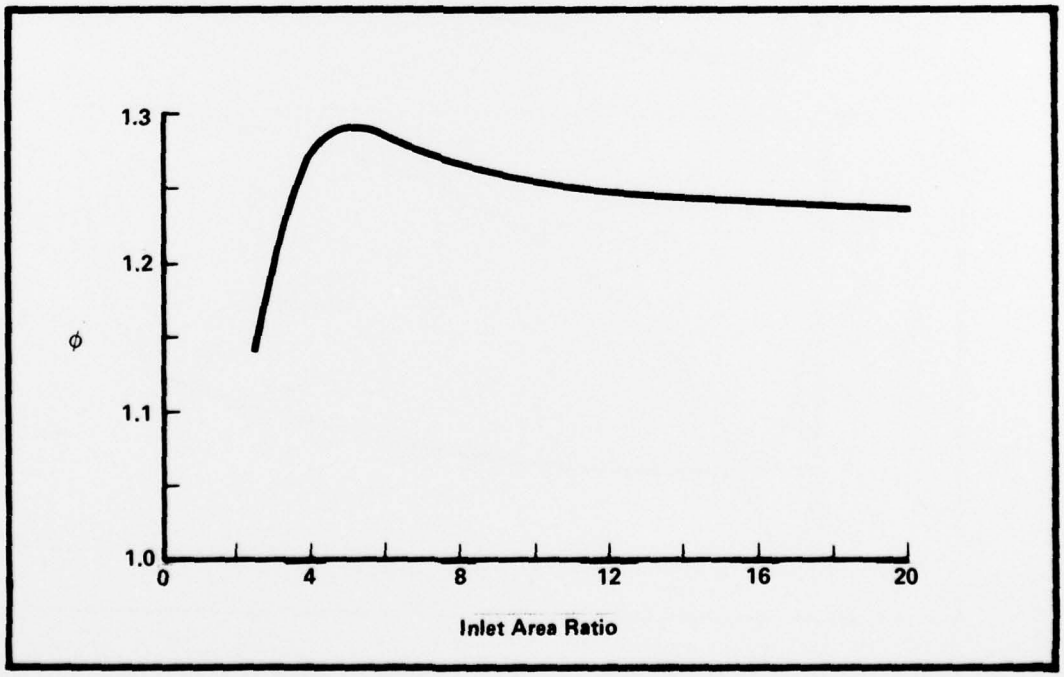

Figure 16. Predicted Effect of Inlet Area Ratio

function of inlet area ratio, for a constant diffuser area ratio of 1.8. The length of the shroud was kept constant, so that the ejector becomes relatively long at low inlet area ratios. In this case the parabolic flow approximation is valid, and the augmentation is seen to initially increase with the inlet area ratio. This is as predicted by the momentum theories. As the sides of the shroud are moved farther apart, the strength and influence of the circulation is diminished, and the augmentation begins to decrease. This is according to the lifting surface theory. Thus, the correct behavior has been predicted in each limit.

CONCLUSIONS

A viscous/inviscid interaction analysis has been used to extend classical momentum theories of ejector thrust augmentation. The primary elliptic effects have been included by iterating between a parabolic solution for the flow through the ejector and an elliptic solution for the flow outside the ejector. Briefly, a calculation of the rate of entrainment by the turbulent jets is used to determine the equivalent sink strengths. The requirement that the ejector shroud must be a streamline of the flow induced by these sinks is then used to evaluate the circulation generated around the shroud. The influence of the circulation is included in the next iteration for the rate of entrainment. Comparison of the calculated thrust augmentation with experimental data establishes confidence in the ability to predict the complex ejector flowfield with this approach. In addition, greater understanding of the principle of ejector thrust augmentation is obtained from the analysis.

The present analysis can be improved by including compressibility and jet temperature effects, and by refining the representation of the flow singularities. More importantly, curvature effects should be added to both the turbulence equations and the mean flow equations in the viscous solution, and additional development of the jet flap diffuser scheme should be undertaken.

APPENDIX I

ELEMENTARY SINK DISTRIBUTIONS

In this Appendix the methods of potential flow theory are used to derive expressions for the velocity induced by elementary sink distributions. This derivation is based on the Douglas method of Hess and Smith.[14] Consider a differential element of a sink distribution located at the point $P(\xi,0)$ and having length $d\xi$, as shown in the sketch. The strength of the sink element is $qd\xi$. In incompressible flow, the magnitude of the velocity induced by the differential sink at a point $P(x,y)$ is

$$V = qd\xi/2\pi r \tag{1}$$

in which r is the distance $\left[(x - \xi)^2 + y^2\right]^{1/2}$. The velocity vector is directed along r, towards the sink. The horizontal and vertical components of the velocity are given by

$$u = V \cos \theta = \frac{qd\xi}{2\pi r} \cdot \frac{(x - \xi)}{r} \tag{2}$$

$$v = V \sin \theta = \frac{qd\xi}{2\pi r} \cdot \frac{y}{r} \tag{3}$$

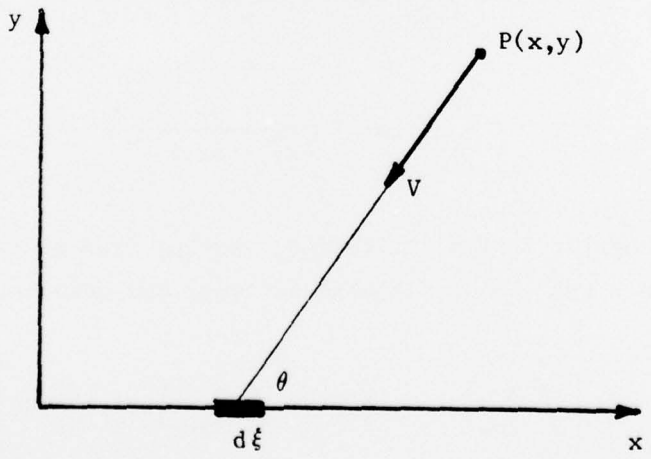

The components of the velocity induced at the point P(x,y) by a sink panel are determined by integrating the contributions of all the elements that make up the panel. For a sink distribution of constant strength per unit length q_j, the horizontal component of velocity is given by:

$$u = \frac{q_j}{2\pi} \int_o^s \frac{(x - \xi)d\xi}{(x - \xi)^2 + y^2}$$

integration of this expression yields

$$u = \frac{q_j}{2\pi} \ln\left[(x - \xi)^2 + y^2\right]^{1/2}\Big|_o^s$$

$$u = \frac{q_j}{2\pi} \ln\left[\frac{(x - s)^2 + y^2}{x^2 + y^2}\right]^{1/2} \qquad (5)$$

Similarly, the vertical component of velocity is given by

$$v = \frac{q_j}{2\pi} \int_o^s \frac{y d\xi}{(x - \xi)^2 + y^2}$$

and integration yields

$$v = \frac{q_j}{2\pi} \tan^{-1}\left(\frac{\xi - x}{y}\right)\Big|_o^s$$

$$v = \frac{q_j}{2\pi} \tan^{-1}\left(\frac{sy}{x^2 - sx + y^2}\right) \qquad (6)$$

For a triangular sink distribution, varying from q_j at $x = 0$ to zero at $x = \pm s$, the horizontal and vertical components of velocity are given by

$$u = q_j\left[\int_{-s}^{o} \frac{x - \xi}{2\pi r^2}\left(1 + \frac{\xi}{s}\right)d\xi + \int_o^s \frac{x - \xi}{2\pi r^2}\left(1 - \frac{\xi}{s}\right)d\xi\right]$$

$$v = q_j\left[\int_{-s}^{o} \frac{y}{2\pi r^2}\left(1 + \frac{\xi}{s}\right)d\xi + \int_{o}^{s} \frac{y}{2\pi r^2}\left(1 - \frac{\xi}{s}\right)d\xi\right]$$

integration of these expressions yields

$$u = \frac{q_j}{2\pi}\left\{\frac{y}{s}\left[\tan^{-1}\left(\frac{sy}{x^2 + sx + y^2}\right) + \tan^{-1}\left(\frac{-sy}{x^2 - sx + y^2}\right)\right]\right.$$

$$\left. + \left(\frac{x}{c} + 1\right)\ln\left(\frac{(x + s)^2 + y^2}{x^2 + y^2}\right)^{1/2} + \left(\frac{x}{s} - 1\right)\ln\left(\frac{(x - s)^2 + y^2}{x^2 + y^2}\right)^{1/2}\right\} \quad (7)$$

and

$$v = \frac{q_j}{2\pi}\left\{\left(\frac{x}{s} + 1\right)\tan^{-1}\left(\frac{sy}{x^2 + sx + y^2}\right) + \left(\frac{x}{s} - 1\right)\tan^{-1}\left(\frac{-sy}{x^2 - sy + y^2}\right)\right.$$

$$\left. - \frac{y}{s}\left[\ln\left(\frac{(x + s)^2 + y^2}{x^2 + y^2}\right)^{1/2} + \ln\left(\frac{(x - s)^2 + y^2}{x^2 + y^2}\right)^{1/2}\right]\right\} \quad (8)$$

By suitable transformation of coordinates, these expressions can be used to calculate the velocity induced by any panel at any other point in the field.

APPENDIX II

SINK ENTRAINMENT VELOCITIES

In this Appendix the velocities at the midpoint of each sink panel are derived in order to relate the sink strength to the entrainment velocity. For a sink distribution having constant strength, q_j, over the interval from -s to s, the vertical component of velocity is given by

$$v = \frac{q_j}{2\pi} \int_{-s}^{s} \frac{y\,d\xi}{(x - \xi)^2 + y^2} \tag{1}$$

integration of this expression gives

$$v = \frac{q_j}{2\pi} \tan^{-1}\left(\frac{2sy}{x^2 + y^2 - s^2}\right) \tag{2}$$

Approaching the midpoint of this panel, first in the limit as $x \to 0$, then along the centerline as $y \to 0$ yields

$$v\ (0,0) = \frac{q_j}{2} \tag{3}$$

Thus, the sink strength per unit length is given by twice the entrainment velocity $q_j = -2V_e$.

For a triangular sink distribution which varies from q_j at its center to zero at each end, the vertical component of velocity is given by Equation (8) of Appendix I. Approaching the midpoint of the panel as before, first in the limit as $x \to 0$, yields,

$$v\ (0,y) = \frac{q_j}{2\pi}\left[\frac{y}{s} \ln\left(\frac{s^2 + y^2}{s^2}\right) + 2 \tan^{-1}\left(\frac{s}{y}\right)\right] \tag{4}$$

along the centerline. Then, as $y \to 0$,

$$v\ (0,0) = \frac{q_j}{2} \tag{5}$$

Thus, the strength of the sink is given by twice the entrainment velocity, $q_j = -2V_e$, in this case also.

REFERENCES

1. Korbacher, G. K., "Aerodynamics of Powered High-Lift Systems," Annual Review of Fluid Mechanics, 1974, pp 319-358

2. von Karman, T., "Theoretical Remarks on Thrust Augmentation," in Contributions to Applied Mechanics, Reissner Anniversary Volume, pub. by J. W. Edwards, Ann Arbor, Mich., 1949, pp 461-468

3. Gilbert, G. B. and Hill, P. G., "Analysis and Testing of Two-Dimensional Slot Nozzle Ejectors with Variable Area Mixing Sections," NASA CR-2251, 1973

4. DeJoode, A. D. and Patankar, S. V., "Prediction of Three-Dimensional Turbulent Mixing in an Ejector," AIAA Journal, Vol. 16, No. 2, February 1978, pp 145-150

5. Quinn, B. P., "Compact Ejector Thrust Augmentation," Journal of Aircraft, Vol. 10, No. 8, Aug. 1973, pp 481-486

6. Bevilaqua, P. M., "Evaluation of Hypermixing for Thrust Augmenting Ejectors," Journal of Aircraft, Vol. 11, No. 6, June 1974, pp 348-354

7. Bevilaqua, P. M., "Lifting Surface Theory for Thrust Augmenting Ejectors," AIAA Journal, Vol. 16, No. 4, April 1978, pp

8. Launder, B. E. and Spalding, D. B., "The Numerical Computation of Turbulent Flows," Computer Methods in Appl. Mech. and Eng., Vol. 3, No. 2, March 1974, pp 269-289

9. Patankar, S. V. and Spalding, D. B., "Heat and Mass Transfer in Boundary Layers," International Textbook Company, Ltd, London, 1970

10. Sparrow, E. M., Baliga, B. R. and Patankar, S. V., "Heat Transfer and Fluid Flow Analysis of Interrupted Wall Channels with Applica-to Heat Exchangers," Journal of Heat Transfer, February 1977, Vol. 99, p 4

11. Morel, J. P. and Lissaman, B. S., "The Jet Flap Diffuser, a New Thrust Augmenting Device," AIAA Paper No. 69-777

12. Spence, D. A., "The Lift Coefficient of a Thin, Jet-Flapped Wing," Royal Society of London, Proceedings, Vol. 238, Jan. 1957, pp 46-

13. Marsters, G. F., "Interaction of Two Plane, Parallel Jets," AIAA Journal, Vol. 15, No. 12, Dec. 1977, pp 1756-1762

14. Hess, J. L. and Smith, A. M. O., "Calculation of Potential Flow About Arbitrary Bodies," Progress in Aeronautical Sciences, Vol. 8, Pergamon Press, New York, 1967

DISTRIBUTION LIST

Office of Naval Research
800 N. Quincy St.
Arlington, VA 22217
- ONR 211 — 4
- ONR 430B — 1

Office of Naval Research Branch Office
1030 E. Green St.
Pasadena, CA 91106 — 1

Office of Naval Research Branch Office
536 South Clark Street
Chicago, IL 60605 — 1

Office of Naval Research Branch Office
Bldg. 114 Section D
666 Summer St.
Boston, MA 02210 — 1

Naval Research Laboratory
Washington, DC 20375
- Code 2627 — 1
- Code 2629 — 1

Defense Documentation Center
Bldg. 5 Cameron Station
Alexandria, VA 22314 — 12

Naval Air Systems Command
Washington, DC 20362
- NAIR 320D (Mr. R. Siewert) — 1
- NAIR 5301 (Mr. R. Weinraub) — 1
- ADPO-14 (CDR E. Lewis) — 1

U. S. Naval Postgraduate School
Monterey, CA 93940
- Dept. of Aeronautics (Code 57) — 1
- Library — 1

David Taylor Naval Ship Research and Development Center
Bethesda, MD 20084
- Code 16 (Dr. H. Chaplin) — 1
- Code 1606 (Dr. T. Tai) — 1
- Code 522.3 Aero Library — 1
- Code 166 (Mr. R. Murphy) — 1

Naval Air Development Center
Warminster, PA 18974
- Code 6053 (Dr. K. Green) — 1

NASA Langley Research Center
Hampton, VA 23665
- Mr. R. Culpepper — 1

NASA Ames Research Center
Moffett Field, CA 94035
- Dr. D. Hickey — 1

Wright Patterson Air Force Base
Dayton, OH 45433
- AFFDL (Dr. K. Nagaraja) — 1

Air Force Office of Scientific Research
Bldg. 410
Bolling AFB, DC 20332
- Code NA (Dr. J. Wilson) — 1

General Dynamics/Fort Worth Division
P. O. Box 748
Fort Worth, TX 76101
- Aero. Section (Dr. W. Foley) — 1

Nielsen Engineering & Research Inc.
510 Clyde Avenue
Mountain View, CA 94043 — 1

McDonnell Douglas Aircraft Co.
P. O. Box 516
St. Louis, MO 63166
- Dept. 241 (Mr. R. Jenny) — 1
- Dept. 230 (Mr. R. McDonald) — 1

Lockheed Missiles & Space Co., Inc.
Huntsville Research & Engineering
P. O. Box 1103
Huntsville, AL 35807
Mr. A. Zalay 1